Conference paper

Zhichang Liu and J. Fraser Stoddart*

Extended metal-carbohydrate frameworks

Abstract: Cyclodextrins (CDs) – a family of cyclic oligosaccharides – are ideal building blocks for the construction of environmentally benign materials. Herein, we reflect upon the serendipitous discovery of two classes of extended crystalline materials – referred to as cyclodextrin metal-organic frameworks (CD-MOFs) and CD-Bamboo – based on CDs which offer opportunities for potential applications in the world of industry and commerce all the way from sequestering carbon dioxide to extracting gold in an eco-friendly manner. The crucial role of serendipity in scientific research expresses itself two times over at the boundaries between coordination chemistry with materials science.

Keywords: crystallization; cyclodextrins; gold extraction; ICS-27; ion recognition; nanoporous coordination polymers; self-assembly.

DOI 10.1515/pac-2014-0303

Introduction

From Archimedes' apocryphal flash of inspiration, while immersed in a bathtub, to Newton's apocryphal moment when the penny dropped while seated under an apple tree, we have inherited two intriguing pieces of folklore in classical physics which demonstrate the all-important roles that serendipity plays in many fundamental scientific discoveries that fuel future technological revolutions. Fortuitous discoveries, which influence our everyday lives, have continued to thrive under the umbrella of 'blue skies' research from time immemorial. In the fields of chemistry, materials science, and medicine, aspartame, cellophane, penicillin, polyethylene, and Teflon® represent but a few of the emergent products and materials made serendipitously [1] while researchers were searching for something quite unrelated. Thanks to serendipity, breakthroughs in the basic sciences have had consequences that reach far beyond the boundaries of any individual field and have resulted in the development of completely new lines of interdisciplinary research.

Cyclodextrins (CDs) are a family of carbohydrates composed of α -1,4-linked D-glucopyranosyl residues, bound together in tori – i.e., cyclic oligosaccharides – which are mass-produced from starch by means of enzymatic conversions in microorganisms. The capability of CDs to act as hosts and form complexes with hydrophobic guests enables them to be applied widely in a broad range of research activities related to supramolecular and pharmaceutical chemistry – not least of all, drug delivery. Recent research by us on CDs with the goal of synthesizing mechanically interlocked molecules (MIMs) [2] has led to the serendipitous discoveries of two classes of extended crystalline materials based on these cyclic oligosaccharides – referred to as cyclodextrin metal-organic frameworks (CD-MOFs) [3] and CD-Bamboo [4] – which hold out prospects for potential applications all the way from sequestering carbon dioxide to extracting gold. The outcomes were

Article note: A collection of invited papers based on presentations at the 27th International Carbohydrate Symposium (ICS-27), Bangalore, India, 12–17 January 2014.

^{*}Corresponding author: J. Fraser Stoddart, Department of Chemistry, Northwestern University, 2145 Sheridan Road, Evanston, IL 60208, USA, e-mail: stoddart@northwestern.edu

Zhichang Liu: Department of Chemistry, Northwestern University, 2145 Sheridan Road, Evanston, IL 60208, USA

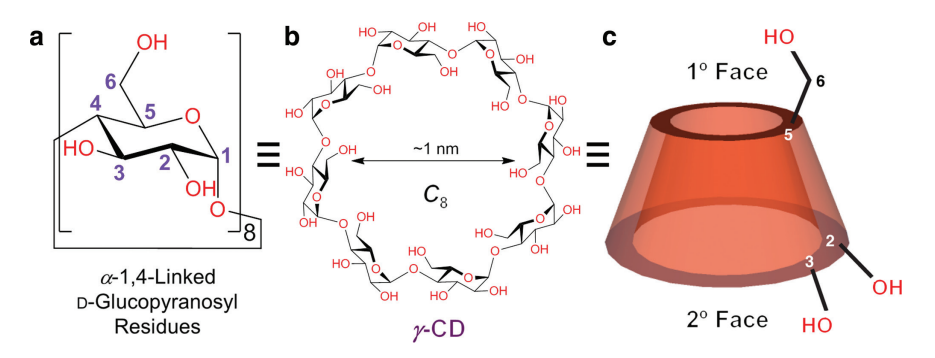


Fig. 1 Structural formulas defining (a) the α -1,4-linked D-glucopyranosyl residues present as a total of eight in (b) γ -cyclodextrin (γ -CD) with its C_8 symmetry. (c) A graphical representation of γ -CD.

unrelated to our initial research goals involving MIMs. Both tales illustrate the vital role played by serendipity at the confluence of coordination chemistry with materials science.

CD-MOF

 γ -CD is (Fig. 1) a C_8 symmetrical cyclic octasaccharide composed of eight asymmetric α -1,4-linked D-glucopyranosyl residues. Its bucket-shaped cavity with an inner diameter of ~1 nm and a depth of ~0.8 nm is capable of hosting simultaneously two aromatic molecules aided and abetted by mutual π - π stacking and hydrophobic interactions. Thus, a ring-in-ring complex, based on a synthetic macrocycle containing two azobenzene moieties and a γ -CD torus, was contemplated and the feasibility of making it was examined (Fig. 2a) at the outset by exploring the possibility of forming a 2:1 host-guest complex precursor from two azobenzene-4,4'-dicarboxylates and one γ -CD. Upon diffusing MeOH vapor into an aqueous solution of dipotassium azobenzene-4,4'-dicarboxylate and γ -CD (molar ratio: 4:1) during ~5 days, orange, cubic single crystals (Fig. 2b) were obtained. Quite unexpectedly, X-ray diffraction (XRD) revealed that, instead of a 2:1 host-guest complex forming between two azobenzene-4,4'-dicarboxylates and one cyclodextrin, only the γ -CD tori, held together by K⁺ ions, crystallizes in a cubic cell of space group *I*432, while the azobenzene-4,4'-dicarboxylate

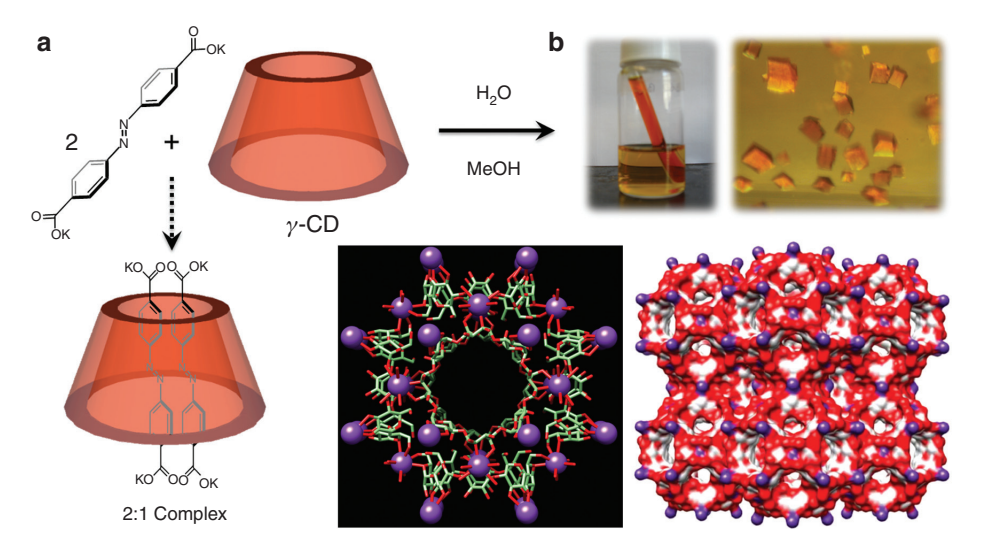


Fig. 2 The serendipitous discovery of CD-MOF-1. (a) Attempts to form a 2:1 complex in aqueous mixture between dipotassium azobenzene-4,4'-dicarboxylate and γ -CD resulted in (b) the formation of cubic crystals of an extended framework called CD-MOF-1 (bottom right) of $(\gamma$ -CD)₆ cubes (bottom left).

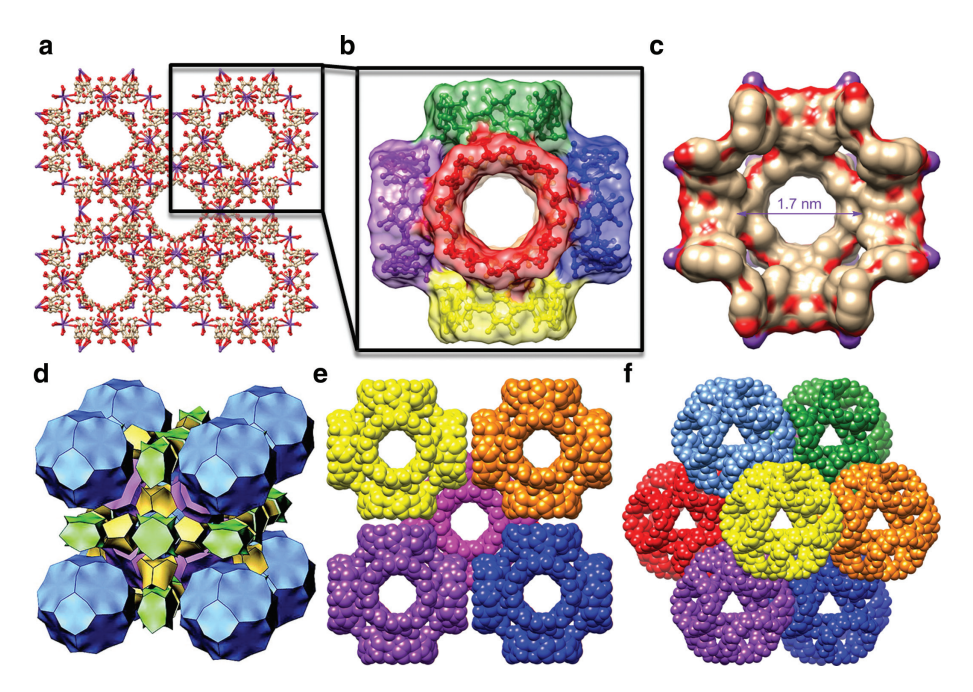


Fig. 3 (a) A ball-and-stick representation of the extended solid-state superstructure of CD-MOF-1, showing the $(\gamma$ -CD), units adopting a body-centered cubic packing arrangement. (b) A cuboidal portrayal of the six γ -CD tori, illustrating (c) the 1.7 nm cavity diameter of each (γ-CD), cube. (d) A computer-generated illustration of the solvent accessible void spaces that are present in the CD-MOF-1 extended structure. (e) A space-filling representation of the extended body-centered cubic packing in the crystal structure of CD-MOF-1, wherein the spherical cavities are connected by cylindrical channels defined by an inner diameter (0.8 nm) of the γ -CD tori. (f) A space-filling representation of CD-MOF-1 viewed down the 111 plane at 45° to each of the crystallographic axes revealing the smaller triangular channels of cross section 0.4 nm.

guest counterions are totally disordered. While the desired outcome was not realized, an infinite nanoporous framework with an extended structure presented itself to us on a plate! On realizing the critical role of the K⁺ ions in the formation of this framework, KOH was used in place of dipotassium azobenzene-4,4'-dicarboxylate with the goal of constructing an isoreticular framework. Following a similar slow vapor diffusion protocol, colorless cubic single crystals - for which we coined the name CD-MOF-1 - were obtained [3] from KOH and γ -CD. As expected, the single crystal XRD analysis revealed (Fig. 3a) that CD-MOF-1 crystallizes in an isostructural cubic cell of space group I432, while the OH- counterions and solvent molecules are disordered throughout the crystalline lattice. Six γ -CD tori assemble (Fig. 3b) into a (γ -CD), cube through coordination of K⁺ ions to the C-6 OH groups and the glycosidic ring O atoms on the inwardly directed primary (1°) faces of alternating D-glucopyranosyl residues around the γ -CD tori, forming a spherical cavity (Fig. 3c) of diameter 1.7 nm. The $(\gamma$ -CD), cubes pack (Fig. 3a) in an infinite body-centered cubic manner through coordination of K⁺ ions to the C-2 and C-3 OH groups of the second set of alternating D-glucopyranosyl residues on the outwardly oriented secondary (2°) faces of the γ -CD tori. The central cavities (Fig. 3d) are linked (Fig. 3e) to each other by the channels (0.8 nm) formed from tail-to-tail γ -CD pairs aligned along the a, b, and c axes in the crystal, connecting, in an infinite manner, the cavities that are also perforated (Fig. 3f) by smaller triangular pores (0.4 nm) directed along the (111) planes in the crystal. It is noteworthy (Fig. 4) that the K⁺ ions not only (i) coordinate to the 1° face of the γ -CD units to form (γ -CD), cubes, but also (ii) link these cubes together to form a three-dimensional extended structure through coordinating to the 2° face of the γ -CD tori. Eight-coordinate K+ ions (Fig. 4b) are generated by this dual linking process, while each individual D-glucopyranosyl residue on a γ -CD torus is coordinated by K⁺ ions in an alternating 1° face/2° face fashion. Although a 2:1 ratio of K⁺ to γ -CD is observed, the number of the counterions is difficult to ascertain on account of the uncertain nature of the ligands – either OH or O⁻ but, most likely the former based on its pK_3 value of 13 – in addition to the fact that the counterions are disordered. The ¹H NMR spectra of two analogues of CD-MOF-1, prepared from γ -CD with (i) potassium benzoate and (ii) dipotassium azobenzene-4,4'-dicarboxylate revealed a 2:1 ratio of benzo-

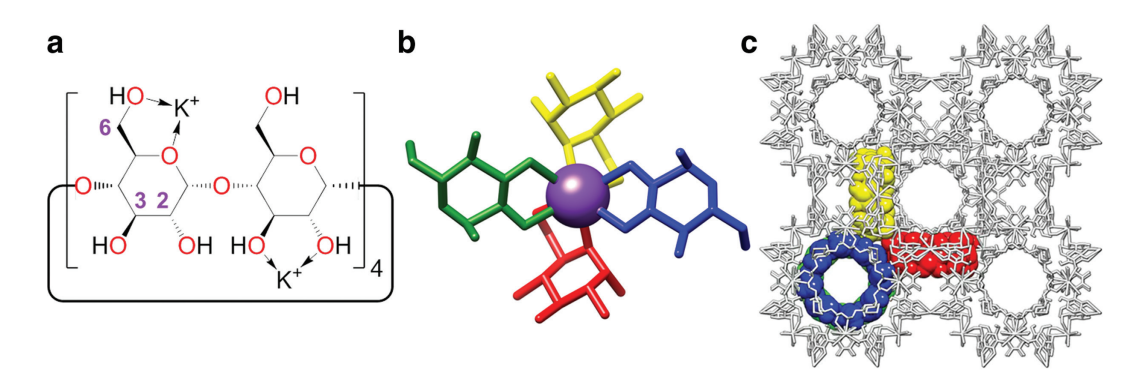


Fig. 4 (a) The alternating arrangement of K⁺ ions coordinated to the 1° and 2° faces of the four repeating maltosyl units within γ -CD in CD-MOF-1. (b) A tubular representation of the coordination of a K⁺ ion (purple sphere) in the solid-state structure of CD-MOF-1. The K⁺ ion coordinates to the secondary OH groups, attached to C-2 and C-3 on two separate D-glucopyranosyl residues (green and blue) while two further residues (yellow and red) are coordinated to the glycosidic ring O atom and the primary OH group attached to C-6. (c) Expanded solid-state superstructure of CD-MOF-1, with four γ -CD tori coordinated to one K⁺ ion displayed as space-filling models in green, blue, yellow, and red colors. The green γ -CD torus is hid by the blue one because of the parallel arrangement of both γ -CD tori along the central axis.

ate anions to γ -CD and a 1:1 ratio for the azobenzene-4,4'-dicarboxylate counterions following dissolution in D₂O, observations, both of which confirm the nature of the ligands to be neutral OH groups.

Isostructural CD-MOF-2 and -3 have also been prepared from γ-CD on gram-scales with RbOH and CsOH, respectively, by following the same procedure as that employed in the preparation of CD-MOF-1. Although the coordination geometries of the K⁺, Rb⁺, and Cs⁺ cations in CD-MOFs 1–3 are very similar, the [M⁺···O] bond lengths increase on going from K⁺ to Rb⁺ to Cs⁺. Isostructural cubic structures with similar unit cell parameters are formed by all the alkali metal cations investigated except lithium. When salts of Na⁺ and Cs⁺ are employed in the preparation of CD-MOFs, extended structures other than the cubic ones, are also formed. In the case of CsOH, needle-shaped crystals - comprised of CD-MOF-4 - which are very different from the cubic crystals of CD-MOF-3, are produced concurrently during the crystallization process. Single crystal XRD reveals CD-MOF-4 to have a channel-type superstructure, comprised of coaxially stacked head-to-tail γ -CD tori linked by Cs⁺ ions, coordinating to form two different channel types. The use of Na⁺ salts also shows counterion dependency. While Na CO, and γ -CD lead to cubic crystals with a unit cell that is isostructural to that of the other CD-MOFs, NaOH with γ -CD forms a channel-like superstructure [(NaOH) $_{\gamma}$ -(γ -CD)], which is different from that of CD-MOF-4. It is noteworthy that the cubic space group I432 with a unit cell edge of ~31 Å has been reported [5] previously for crystals obtained from Na⁺ ions and γ-CD. Both cubic orange and colorless single crystals were obtained, respectively, by adding an ethanolic solution of NaOH to DMF solutions, one containing γ -CD and FeCl, and the other, γ -CD and NaCl. Although the authors identified a unit cell similar to that of CD-MOF-1 in both cases, they were unable to refine the data and obtain the solid-state structures. We suspect that these crystals were isostructural with the cubic CD-MOFs.

The successful preparation of CD-MOFs from γ -CD and Group IA metal cations aroused our curiosity in relation to the Group IIA alkaline earth metal cations. Only γ -CD and SrBr $_2$ have given [6] (in very low yield) crystals suitable for single crystal XRD analysis. The solid-state superstructure of $[(SrBr_2)\cdot(\gamma$ -CD)]_n reveals a totally different topology from the cubic and the channel-type extended structures obtained with the alkali metal cations. The γ -CD tori are assembled in a trigonal "offset stack" manner. Inspection of the structure of $[(SrBr_2)\cdot(\gamma$ -CD)]_n reveals that the Sr 2 + dications are nine-coordinated by three water molecules and three γ -CD units. It has been reported [7] that β -CD and MgCl $_2$ can be crystallized as $[(Mg(H_2O)_6Cl_2)_2\cdot\beta$ -CD] in which the Mg 2 + cations are completely hydrated and so do not coordinate with any portion of the β -CD tori. Other examples of crystalline complexes between alkaline earth metals and CDs include [β -CD-2CaCl $_2$ -11.25H $_2$ O] [8] and [α -CD-3CaCl $_2$ -19H $_2$ O] [9]. A common feature of these complexes is the fact that the alkaline earth metal dications are partially or completely hydrated.

Although γ -CD is a chiral building block, no superstructures with induced chiralities have so far been reported in the literature. α -CD, however, forms with RbOH an extended porous superstructure, whose CD

metal-carbohydrate framework displays [10] left-handed helicity. Single crystal XRD analysis reveals that the helical superstructure is created by the coordination of Rb $^{\circ}$ ions to the 1° and 2° faces of the α -CD tori. The chirality of the α -CD tori induces this supramolecular helicity in the CD metal-carbohydrate framework in the solid state.

Strong uptake of CO₂

Thermogravimetric analysis (TGA) and powder XRD (PXRD) reveal that crystals of CD-MOF-1 and -2 are stable and display permanent porosity as evidenced by their ability to retain their crystallinity, even after evacuation. A long-term examination during several months reveals that the crystals of CD-MOF-2 have the higher stability of the two. The permanent porosities of the evacuated CD-MOF-1 and -2 have been demonstrated by measuring N₂, H₃, CO₂, and CH₄ adsorptions. The isotherms for N₂ show a steep uptake in the $P/P_0 < 0.05$ regions at 77 K, indicative of the nanoporosities of these frameworks. The BET (Langmuir) surface areas of CD-MOF-1 and -2 are estimated to be 1220 (1320) and 1030 (1110) m² g⁻¹, respectively, corresponding to a density of 0.47 g cm⁻³. CD-MOF-2 also shows [11, 12] a steep uptake in the low-pressure region of its CO₂ isotherm recorded at 298 K, an observation which reveals an strong binding between CO₂ and the extended framework. In order to gain insight into the nature of the adsorption process, variable temperature isotherms were measured (Fig. 5a) for both CO, and CH, with CD-MOF-2. Changing the temperature from 273 to 298 K did not affect the uptake of CO, in the <1 Torr region, while a knee point at ~23 cm³ g⁻¹ was observed at all temperatures. A nearly 3000-fold selectivity for CO₂ over CH₄ was also observed in the low-pressure region. The strong CO, binding revealed by the steep uptake in the low-pressure region can be ascribed to the formation of a covalent bond – that is, chemisorption. It is noteworthy that the sharp turn in the >1 Torr high-pressure region is temperature dependent, indicative of a physisorption process in this region. The complete adsorption mechanism can be interpreted [11, 12] as (i) a chemisorption process in the <1 Torr region with a capacity of <23 cm³ g⁻¹, followed by (ii) a physisorption process in the >1 Torr region with a capacity of >23 cm³ g⁻¹. Cross-polarized magic-angle-spinning (CP/MAS) ¹³C NMR spectroscopy provided further evidence for the chemisorptive process. A new resonance which appears at 158 ppm upon exposure of a sample of CD-MOF-2

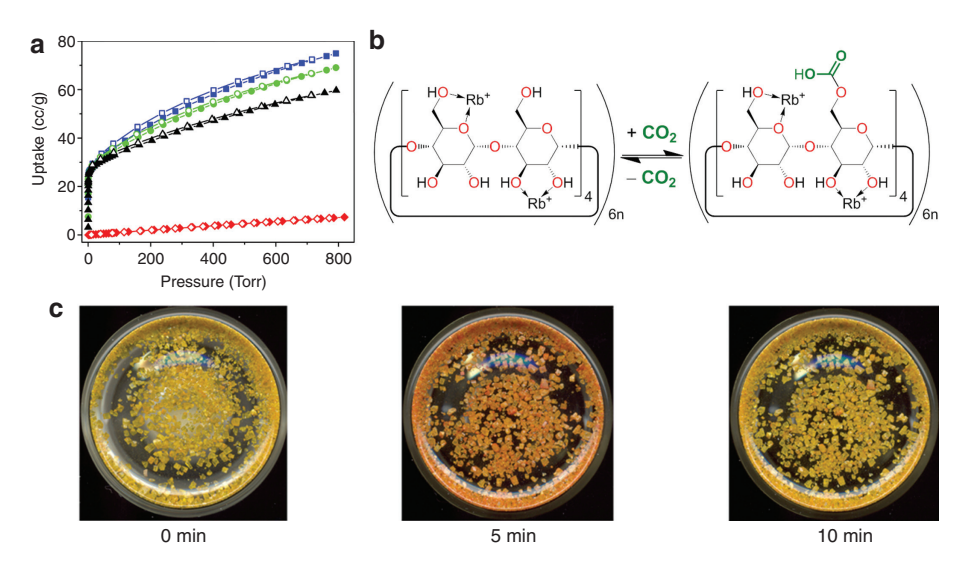


Fig. 5 (a) Gas adsorption isotherms for activated CD-MOF-2, indicating the uptake of CO, measured at 273 K (blue), 283 K (green), and 298 K (black) to be contrasted with the uptake of CH, at 298 K (red). (b) Schematic diagram illustrating the equilibrium proposed to exist during the chemisorption of CO, by CD-MOF-2. (c) Photographs of activated CD-MOF-2 samples doped with methyl red at selected time intervals during CO, sorption and desorption processes. Left: Yellow crystals prior to CO, exposure. Middle: Red crystals obtained after exposure of the yellow crystals to CO, for 5 min. Right: Crystals that reverted back to yellow following removal of the CO, atmosphere, allowing air to enter the vial over 5 min.

to CO₂ indicates the formation (Fig. 5b) of carbonic acid functions, most likely associated with the primary hydroxyl groups on the γ -CD tori. We suspect that the large local CO, concentration inside the cavities of CD-MOF-2 promotes the formation of these carbonic acid functions. Since γ -CD by itself does not react with CO₂, we are evidently witnessing an example of emergent behavior in the case of CD-MOF-2. Direct visible evidence for the formation of carbonic acid functions in CD-MOF-2 has been obtained by doping crystals with a pH indicator (methyl red). Regardless of whether the CO₂ is wet or dry, the color of the crystals changes (Fig. 5c) from yellow to red upon exposing them to CO₂. Removing the supply of CO₂ results in a change in color of the crystals from red to yellow. This reversible process can be repeated more than 10 times. These observations are commensurate with the operation of Le Chatelier's principle during the formation and cleavage of carbonic acid functions associated with the primary hydroxyl groups of the γ -CD tori in CD-MOF-2. Direct adsorption calorimetry reveals [13] that the enthalpy of CO₂ adsorption by CD-MOF-2 displays both chemi- and physisorptive characteristics.

Edible CD-MOF-1

Although MOFs – extended structures composed of secondary building units (SBUs) and organic ligands – have been identified [14] as promising materials with broad potential applications in gas adsorption and separation science, as well as in catalysis and sensor technology, a large number of these original MOFs are composed of toxic transition metals and nondegradable organic ligands. Since they are environmentally benign, the CD-MOFs are appealing [15] from the viewpoint of sustainable development. Their discovery has made edible MOFs a reality. Upon diffusing high proof grain ethanol (Everclear) into an aqueous mixture of food grade γ-CD and potassium benzoate (a common preservative, E212) for 2–7 days, edible CD-MOF-1 has been isolated (Fig. 6) from naturally occurring starting materials. This edible MOF is isostructural with the other CD-MOFs and exhibits similar properties. The safe, cheap, easily made features of edible CD-MOF-1 demonstrate its potential in industries, such as those concerned with food and personal care, in addition to the home care and pharmaceutical industries.

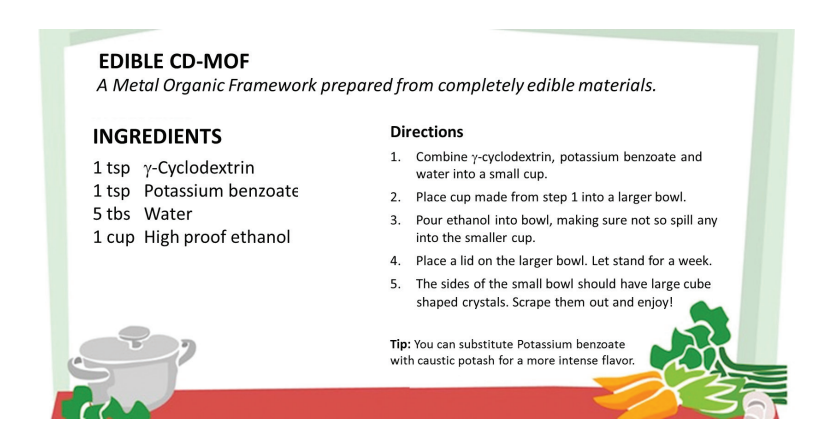


Fig. 6 A recipe for making CD-MOF-1 in the kitchen.

Applications

The robust crystallinity and porosity of CD-MOF-2 render it a potential sensor in principle. A series of micropatterns of pH- and photo-responsive dyes and indicators have been imprinted [16] into crystals of CD-MOF-2 by employing a MeOH-compatible agarose gel stamp. The micropattern-imprinted crystals show pH- or photoresponsive color changes that could herald the development of MOF-based sensors [17] and memristors [18]. Taking advantage of the cavities of diameter 1.7 nm and the high local concentrations of the OH⁻ ions, a

CD-MOF-based template strategy has been developed [19] for the syntheses of silver and gold nanoparticles, as well as core/shell architectures, starting with AgNO, and HAuCl, as precursors. The Ag and Au precursors diffuse into the crystals to be reduced by the OH⁻ ions, forming nanoparticles which can be released readily, simply by dissolving the γ -CD-MOF crystals in water. It should be mentioned that a similar strategy has been reported by Gatteschi and coworkers [5]. Although these researchers were unable to identify the precise structure of crystals grown from an aqueous mixture of γ -CD, FeCl,, and NaOH, XRD data revealed that their solid-state structure is isostructural with those of CD-MOFs. Uniformly dispersed γ -Fe₃O₃ nanoparticles with average diameters of 1.8 nm were found to be generated inside the crystals. The large cavities inside CD-MOFs have also been used [20] to host and stabilize [Ru(bpy)]Cl,, a nanosized photocatalyst, that otherwise would be photodegraded in an unconfined atmosphere. The existence of numerous free hydroxyl groups on the γ -CD tori of CD-MOFs, not only facilitates the strong CO₃ uptake, but also allows the cross-linking between these hydroxyl groups with appropriate reagents to produce gel particles. Well-defined cubic polymer gels can be prepared [21] from a CD-MOF-1 template through cross-linking with ethylene glycol diglycidyl ether and then removing the metal ions. These gels are bio-degradable and can potentially be used in biomedical applications such as drug delivery. Recently, the potential of edible CD-MOF-1 as a drug carrier has been explored [22] by grand canonical Monte Carlo (GCMC) simulations. The adsorption isotherm for ibuprofen in CD-MOF-1 exhibits two steps in which (i) the molecules are first of all adsorbed in the cylindrical channels of ~8 Å diameter, and then (ii) the large cavities of 1.7 nm in diameter are saturated with the molecules. In particular, a controlled release process involving CD-MOF-1 can be inferred on account of its high energy of adsorption.

It is obvious, on reflection, that the reason γ -CD forms (γ -CD) cubes, which themselves act as building blocks in the formation of the extended structures of CD-MOFs, lies in the eight-fold symmetry of γ -CD. This element of symmetry commutes with C_{λ} symmetry, which lies at the heart of the formation of the CD-MOFs. β -CD, which has C, symmetry, shows no propensity to form extended metal-carbohydrate frameworks.

CD-Bamboo

CD-MOFs which were synthesized serendipitously from γ -CD and alkali salts have revealed a new class of nanoporous metal-carbohydrate frameworks that displays unique properties. The fact that isostructural CD-MOFs can be made from Na⁺, K⁺, Rb⁺, and Cs⁺ salts with various counterions including OH⁻, F⁻, Cl⁻, Br⁻, BPh_{h}^{-} , CO_{3}^{2-} , $PhCO_{3}^{-}$, and azobenzene-4,4'-dicarboxylate etc., in a highly reproducible fashion suggested initially to us the seemingly unimportant role of the counterions in the formation of CD-MOFs. When the anions are square-planar tetrahaloaurate anions ($[AuX_{.}]^{-}$ where X = Cl or Br), however, yet another tale of serendipity emerges on the scene.

Supramolecular polymerization between potassium tetrabromoaurate and α -CD

In an experiment using γ -CD and KAuBr, to make new CD-MOFs, instead of producing an extended cubic framework, γ -CD and [K(OH₂)₆][AuBr₄] co-crystallize [4] into a bamboo-like one-dimensional (1D) superstructure - for which we have coined the term, CD-Bamboo - forming a tetragonal unit cell in which an infinite γ -CD channel is segmented into three CD-containing capsules by the horizontal-oriented square-planar [AuBr_a]⁻ anions. More surprisingly, upon adding an aqueous solution of KAuBr_a into an aqueous solution of α -CD, a shiny pale brown precipitate forms (Fig. 7a) in several minutes. Further experiments with the other five aqueous mixtures between KAuCl_a and KAuBr_a with α -, β -, or γ -CDs revealed (Fig. 8) that this co-precipitation happens only in the case of the aqueous mixture of KAuBr, and α -CD. This serendipitous discovery, which is reminiscent [23, 24] of the precipitation of the second-sphere adduct [{Cu(NH₂)_o(H₂O)}·18C6]_o[PF_e]_{oo}, suggests the formation of an insoluble supramolecular polymer from KAuBr, and α -CD. Scanning electron

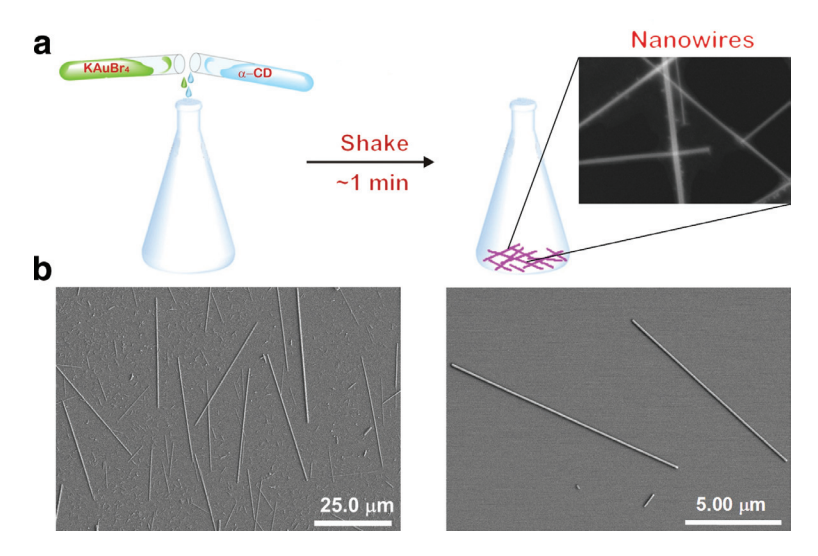


Fig. 7 (a) Formation of crystalline nanowires of the co-precipitated α -Br from KAuBr₄ and α -CD. (b) SEM images of a co-precipitate sample of α -Br.

microscopy (SEM) and transmission electron microscopy (TEM) reveal (Fig. 7b) that the fresh co-precipitates are composed of high aspect-ratio thin needles with diameters of several hundreds of nanometers and lengths of up to several tens of micrometers. Selected area electron diffraction (SAED) patterns also reveal the crystalline nature of the needles. These observations imply that KAuBr₄ and α -CD are able to co-precipitate (Fig. 8) from water in a highly specific manner. In order to gain further insight into the detailed structure of the needles, single crystals were grown from a dilute aqueous mixture of KAuBr₄ and α -CD by the slow vapor diffusion method. X-Ray crystallography of the crystals revealed (Fig. 9) that a second-sphere supramolecular polymer with an infinite chain superstructure {[K(OH₂)₆][AuBr₄] \subset (α -CD)₂}_n – termed α -Br – self-assembles in an orthorhombic space group P2,2₁2. In the asymmetric unit, a distorted, octahedrally coordinated hexa-

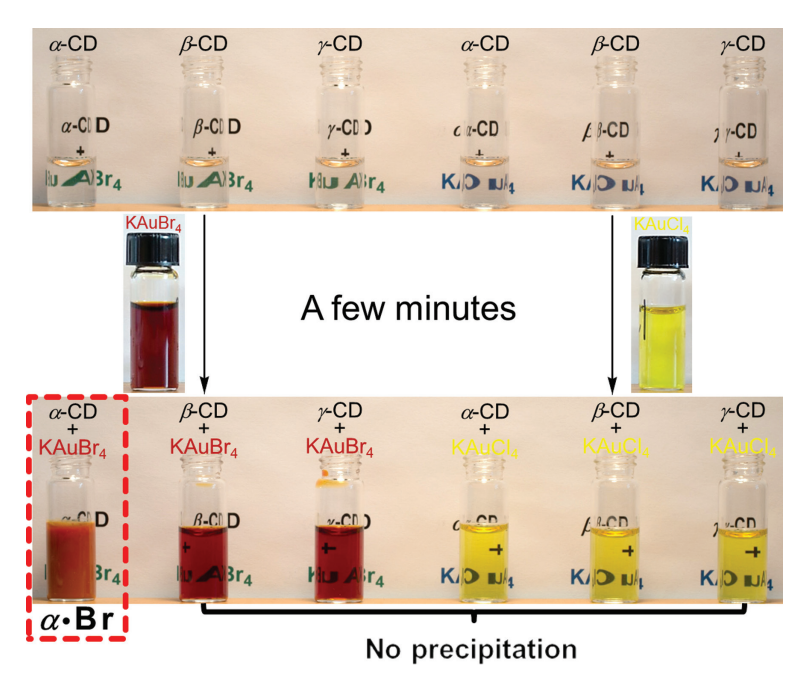


Fig. 8 A comparison of vials illustrating the selective co-precipitation of α -Br from KAuBr, and α -CD.

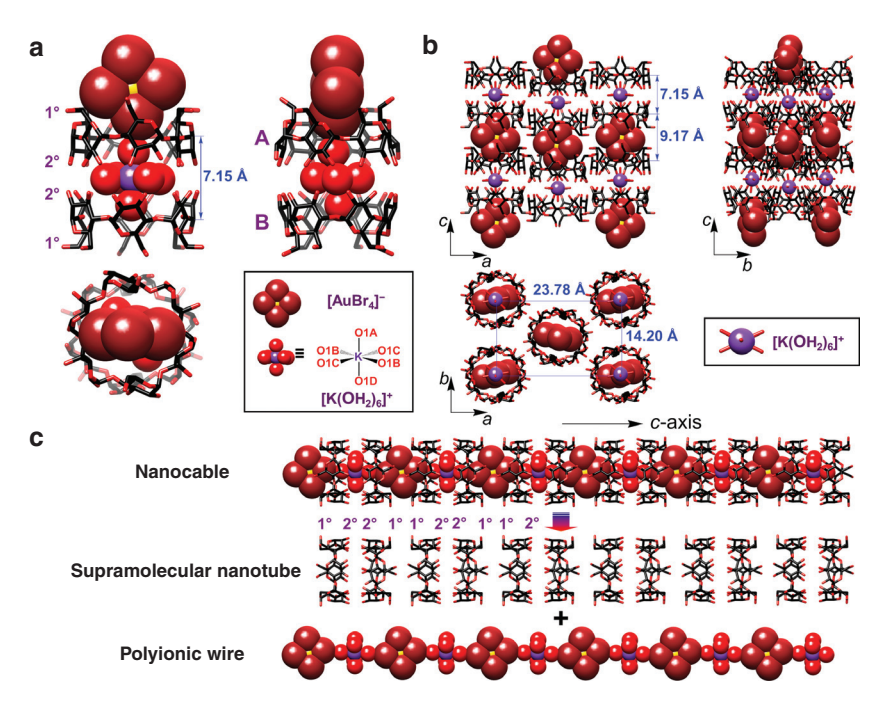


Fig. 9 (a) The single-crystal X-ray structure of $\alpha \cdot Br$. (b) Three views of the crystal packing in the case of $\alpha \cdot Br$. (c) Dissection of one-dimensional nanocable-like superstructure of $\alpha \cdot Br$.

aqua potassium cation $[K(OH)_{\alpha}]^+$ is encapsulated (Fig. 9a) in the cavity of a tail-to-tail α -CD dimer, while the square-planar [AuBr_a] anion is included in the cavity formed between two head-to-head α -CD tori. The [O-H···O-H] hydrogen bonding and van der Waals interactions between [K(OH,),] and the OH groups on the 2° faces of the α -CDs contribute to the stabilization of the hydrophilic [K(OH₃)₆]⁺ in the hydrophobic α -CD dimer cavity. The vertically oriented [AuBr,] anions are stabilized by the [C-H···Br-Au] hydrogen bonds with lengths of 2.92–3.19 Å between [AuBr_c] with H-5 and H-6 on the 1° faces of α -CDs. The co-axial stacking of these units along the c-axis with the aid of multiple hydrogen bonding, van der Waals interactions, and Columbic interactions gives rise (Fig. 9c) to an infinite cable-like superstructure in which the head-to-head and tail-to-tail aligned α -CD channels are filled up by ion chains comprised of $[K(H,0)_{\epsilon}]^+$ and $[AuBr_{\epsilon}]^-$ in an alternating fashion. In particular, the longitudinal O–Br distances between [K(H,O),] and [AuBr,] are <3.4 Å, an observation which implies strong $[O-H\cdots Br-Au]$ hydrogen bonding between $[K(H,O)_c]^+$ and $[AuBr_a]^-$. The purity and the coherence of the crystalline phases in both single crystals and co-precipitates were con-

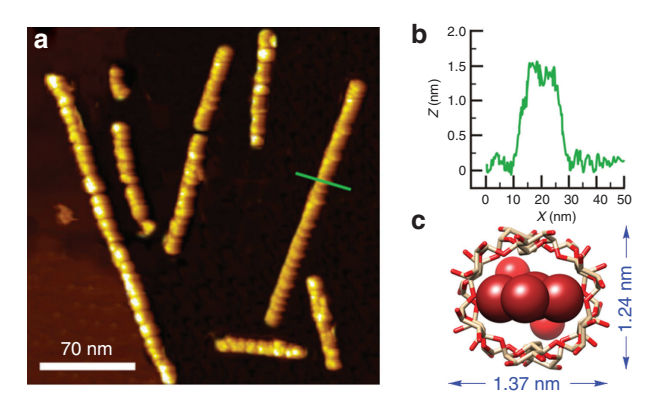


Fig. 10 (a) AFM images of single molecular wires of α -Br grown on a mica surface. (b) The cross-sectional analysis of (a). (c) Dimensions of the cross-section of the one-dimensional α -CD channel in α -Br.

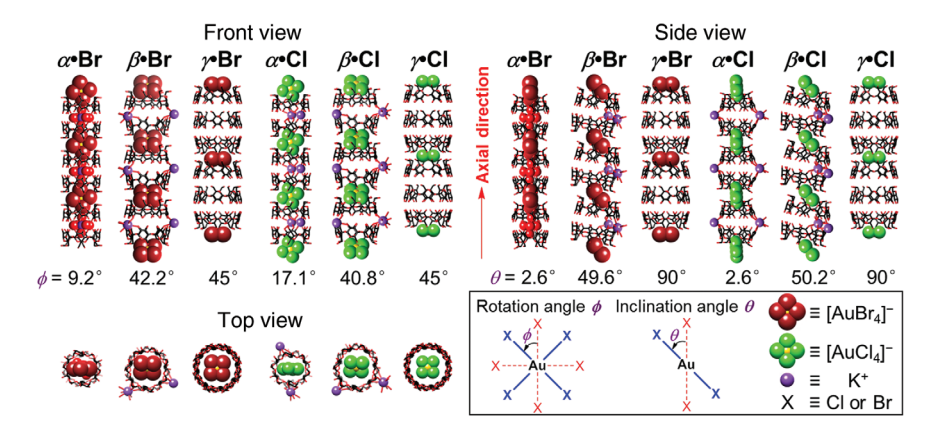


Fig. 11 Bamboo-like single crystal superstructures of α -Br, α -Cl, β -Br, β -Cl, γ -Br, and γ -Cl.

firmed by the perfect match between the experimental PXRD pattern of the as-prepared co-precipitate and the simulated pattern derived from single-crystal XRD data from α -Br. It is worthy of note that there are ca. 4000 1D supramolecular nanoassemblies in a 100 nm diameter co-precipitated needle. The high efficiency of the self-assembly process is revealed by AFM images (Fig. 10) of a spin-coated sample through observing discrete nanoassemblies with lengths of several hundreds of nanometers and heights of ~1.3 nm, a dimension which corresponds to the outer diameter (~1.4 nm) of the α -CD torus.

Potassium tetrahaloaurate complexes with α -, β -, and γ -CDs

In order to gain a deeper understanding of the reasons behind the highly selectively co-precipitated α -Br. single crystals were obtained for all the other aqueous mixtures between KAuX, and CDs through similar slow vapor diffusion procedures and subjected to XRD analysis. X-Ray crystallography of these crystals reveals (Fig. 11) a family of 1D bamboo-like superstructures (CD-bamboo) with structural formulas KAuCl. $(\alpha$ -CD), $KAuBr_{\lambda}\cdot(\beta-CD)_{\gamma}$, $KAuCl_{\lambda}\cdot(\beta-CD)_{\gamma}$, $KAuBr_{\lambda}\cdot(\gamma-CD)_{\beta}$, and $KAuCl_{\lambda}\cdot(\gamma-CD)_{\beta}$ abbreviated as $\alpha\cdot Cl$, $\beta\cdot Br$, $\beta\cdot Cl$, $\gamma\cdot Br$, and γ -Cl, respectively. By comparing all six superstructures, we found that the common features are that the CD tori are stacked along the longitudinal direction to form infinite CD channels which are segregated into isolated capsules by the [AuX₄] anions through [C-H···X-Au] hydrogen bonds. The most obvious difference is that the capsules in α ·Br are filled by second-sphere coordinated [K(OH₂)] to form a highly compact superstructure. Although the only difference between $\alpha \cdot Br$ and $\alpha \cdot Cl$ is that the Au–Cl bond length in $\alpha \cdot Cl$ is 0.15 Å shorter than the Au–Br bond, the K⁺ ions in α ·Cl are located outside the channel and coordinated to the secondary hydroxyl groups on the 2° faces of the α -CD tori. By contrast, β -Br and β -Cl, as well as γ -Br and γ ·Cl, are both isostructural because of the larger diameters of CD tori that diminish the effect of sizes of the [AuX] anions. In the cases of α ·Cl, β ·Br and β ·Cl, the K⁺ ions are coordinated to the 2° faces of the α -CD tori to form 1D latitudinal metal-coordinated polymers. The K⁺ ions in γ -Br and γ -Cl are disordered over the outside channels and are not coordinated. With increasing size of the CD tori, the orientations of [AuBr₄] and [AuCl₄] display a tendency to tilt (Fig. 11). The inclination angle of the $[AuX_{\alpha}]^{-1}$ anion changes from 2.6° in α -CD, and ~50° in β -CD, to 90° in γ -CD.

The surface areas and porosities of all activated samples were analyzed by CO_2 adsorption at 273 K. The isotherms reveals that the BET surface area of $\alpha \cdot Br$ is 35 m² g⁻¹, by far the lowest one because of its compact superstructure devoid of empty capsules. $\alpha \cdot Cl$, $\beta \cdot Br$, and $\beta \cdot Cl$ show modest uptakes and comparable BET surface areas on account of their stable empty cavities. The BET surface areas of $\gamma \cdot Br$ and $\gamma \cdot Cl$ are low simply because the samples become amorphous on evacuation. These observations are well consistent with the results obtained from single crystal XRD and PXRD.

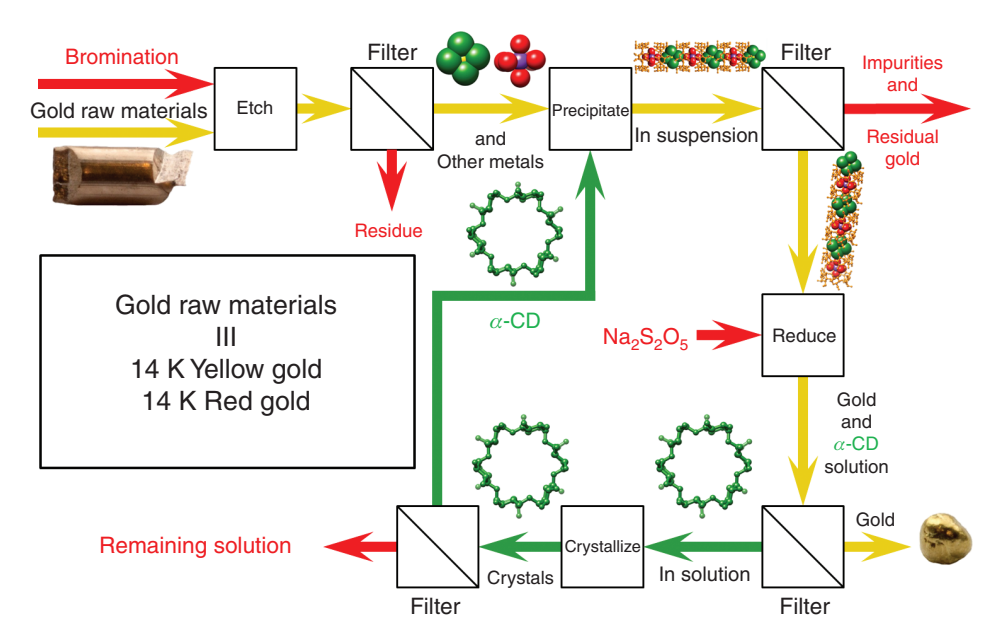


Fig. 12 A flow chart summarizing an improved process which relies on using KBr and Br, to recover gold. The effluent streams are marked in red along with the reagent inputs.

Environmentally benign isolation of gold

The amount of gold production worldwide in 2012 was ca, 2700 tons, of which approximately 83 %, i.e., 2241 tons, are produced by a long-standing cyanidation process [25]. Poisonous cyanides can result in contamination of the environment from accidental leakages and exposures. An environmentally benign method for gold recovery is highly desirable for sustainable development of the environment.

The highly selective precipitation of [AuBr_a] by second-sphere coordination of α -CD – a cyclic oligosaccharide derived from starch - offers a potentially green method for the isolation of gold. This high selectivity of α -CD for [AuBr_s] has proved to be robust in aqueous solution even in the presence of other square planar $[PtX_{\lambda}]^{2-}$ and $[PdX_{\lambda}]^{2-}$ (X = Cl, Br) anions. A laboratory scale process for the highly selective extraction of gold from gold alloys with a gold content of 58 % has been devised [4], based on the precipitation of the α -Br complex. In the primary process, the gold alloys are etched by using Aqua Regia (conc HBr/HNO₃ = 3:1) and then neutralized with KOH to form KAuBr_a. Realizing the corrosive nature of the Aqua Regia that is not environmentally benign, an aqueous mixture of KBr and Br., which is less toxic, and relatively safe and easy to handle, has been used (Fig. 12) to etch the gold-bearing materials and to convert gold to KAuBr, in one step. Our article published [4] in Nature Communications on May 14, 2013 has been viewed by more than 42,000 readers and highlighted in many news outlets throughout the world, a situation which indicates that all over the world there are people who are eager to identify an environmentally benign method to replace the current cyanidation process. The development of a scaled-up process for extracting gold is under investigation in our laboratory.

Conclusions

In summary, given CD-MOFs and CD-Bamboo obtained by two consecutive unforeseen self-assembling occurrences, the crucial role of serendipity in aiding and abetting the development of cyclodextrin chemistry more than 120 years after the discovery of CDs is evident. Only after the fortuitous events do we recognize the importance of these serendipitous discoveries as we explore the properties and develop the potential applications of both CD-MOFs and CD-Bamboo for gas sequestration and environmentally benign gold recovery, respectively. It is conceivable that serendipity will continue to play a major role in enriching science and driving technology forward.

References

- [1] E. L. Eliel. Science and Serendipity: The Importance of Basic Research. American Chemical Society (1992).
- [2] L. Fang, M. A. Olson, D. Benitez, E. Tkatchouk, W. A. Goddard III, J. F. Stoddart. Chem. Soc. Rev. 39, 17 (2010).
- [3] R. A. Smaldone, R. S. Forgan, H. Furukawa, J. J. Gassensmith, A. M. Z. Slawin, O. M. Yaghi, J. F. Stoddart. *Angew. Chem. Int. Ed.* **49**, 8630 (2010).
- [4] Z. Liu, M. Frasconi, J. Lei, Z. J. Brown, Z. Zhu, D. Cao, J. Iehl, G. Liu, A. C. Fahrenbach, Y. Y. Botros, O. K. Farha, J. T. Hupp, C. A. Mirkin, J. F. Stoddart. *Nat. Commun.* 4, 1855 (2013).
- [5] D. Bonacchi, A. Caneschi, D. Dorignac, A. Falqui, D. Gatteschi, D. Rovai, C. Sangregorio, R. Sessoli. *Chem. Mater.* **16**, 2016 (2004).
- [6] R. S. Forgan, R. A. Smaldone, J. J. Gassensmith, H. Furukawa, D. B. Cordes, Q. Li, C. E. Wilmer, Y. Y. Botros, R. Q. Snurr, A. M. Z. Slawin, J. F. Stoddart. J. Am. Chem. Soc. 134, 406 (2012).
- [7] I. Nicolis, A. W. Coleman, P. Charpin, C. de Rango. Angew. Chem. Int. Ed. Engl. 34, 2381 (1995).
- [8] I. Nicolis, A. W. Coleman, P. Charpin, C. de Rango. Acta Crystallogr. B 52, 122 (1996).
- [9] I. Nicolis, A. W. Coleman, M. Selkti, F. Villain, P. Charpin, C. de Rango. J. Phys. Org. Chem. 14, 35 (2001).
- [10] J. J. Gassensmith, R. A. Smaldone, R. S. Forgan, C. E. Wilmer, D. B. Cordes, Y. Y. Botros, A. M. Z. Slawin, R. Q. Snurr, J. F. Stoddart. *Org. Lett.* **14**, 1460 (2012).
- [11] J. J. Gassensmith, H. Furukawa, R. A. Smaldone, R. S. Forgan, Y. Y. Botros, O. M. Yaghi, J. F. Stoddart. J. Am. Chem. Soc. 133, 15312 (2011).
- [12] Y. Liu, Z. U. Wang, H.-C. Zhou. *Greenhouse Gases Sci. Technol.* **2**, 239 (2012).
- [13] D. Wu, J. J. Gassensmith, D. Gouvêa, S. Ushakov, J. F. Stoddart, A. Navrotsky. J. Am. Chem. Soc. 135, 6790 (2013).
- [14] O. M. Yaghi, M. O'Keeffe, N. W. Ockwig, H. K. Chae, M. Eddaoudi, J. Kim. Nature 423, 705 (2003).
- [15] I. Imaz, M. Rubio-Martinez, J. An, I. Sole-Font, N. L. Rosi, D. Maspoch. Chem. Commun. 47, 7287 (2011).
- [16] S. Han, Y. Wei, C. Valente, R. S. Forgan, J. J. Gassensmith, R. A. Smaldone, H. Nakanishi, A. Coskun, J. F. Stoddart, B. A. Grzybowski. *Angew. Chem. Int. Ed.* **50**, 276 (2011).
- [17] J. J. Gassensmith, J. Y. Kim, J. M. Holcroft, O. K. Farha, J. F. Stoddart, J. T. Hupp, N. C. Jeong. J. Am. Chem. Soc. 136, 8277 (2014).
- [18] S. M. Yoon, S. C. Warren, B. A. Grzybowski. Angew. Chem. Int. Ed., 53, 4437 (2014).
- [19] Y. Wei, S. Han, D. A. Walker, P. E. Fuller, B. A. Grzybowski. Angew. Chem. Int. Ed. 51, 7435 (2012).
- [20] S. Han, Y. Wei, B. A. Grzybowski. Chem. Eur. J. 19, 11194 (2013).
- [21] Y. Furukawa, T. Ishiwata, K. Sugikawa, K. Kokado, K. Sada. Angew. Chem. Int. Ed. 51, 10566 (2012).
- [22] M. C. Bernini, D. Fairen-Jimenez, M. Pasinetti, A. J. Ramirez-Pastor, R. Q. Snurr. J. Mater. Chem. B 2, 766 (2014).
- [23] H. M. Colquhoun, J. F. Stoddart, D. J. Williams. Angew. Chem. Int. Ed. Engl. 25, 487 (1986).
- [24] Z. Liu, S. T. Schneebeli, J. F. Stoddart. Chimia 68, 315 (2014).
- [25] T. Norgate, N. Haque. J. Clean. Prod. 29-30, 53 (2012).